In-vacuum Faraday isolation remote tuning

Accadia, T.; Bulten, H.J.; Rabeling, D.S.; van den Brand, J.F.J.; van der Putten, S.

published in
Applied Optics
2011

DOI (link to publisher)
10.1364/AO.49.004780

document version
Publisher's PDF, also known as Version of record

In-vacuum Faraday isolation remote tuning

The Virgo Collaboration[1]

[1]See Appendix A for full list of authors and affiliations.

*Corresponding author: E. Genin (eric.genin@ego-gw.it)

Received 29 April 2010; accepted 5 July 2010;
posted 14 July 2010 (Doc. ID 127707); published 27 August 2010

In-vacuum Faraday isolators (FIs) are used in gravitational wave interferometers to prevent the disturbance caused by light reflected back to the input port from the interferometer itself. The efficiency of the optical isolation is becoming more critical with the increase of laser input power. An in-vacuum FI, used in a gravitational wave experiment (Virgo), has a 20 mm clear aperture and is illuminated by an almost 20 W incoming beam, having a diameter of about 5 mm. When going in vacuum at 10^{-6} mbar, a degradation of the isolation exceeding 10 dB was observed. A remotely controlled system using a motorized $\lambda/2$ waveplate inserted between the first polarizer and the Faraday rotator has proven its capability to restore the optical isolation to a value close to the one set up in air. © 2010 Optical Society of America

OCIS codes: 140.6810, 230.2240.

1. Introduction

In all currently operated gravitational wave (GW) interferometers [1–4], the stability of the beam entering into the interferometer is disturbed by the main back reflection of all the interferometer optics toward the interferometer input port. The light power coming back from the Virgo interferometer is a large fraction of the input light because this interferometer is designed to work on their dark fringe. Faraday isolators (FIs) are therefore placed on the external (in air) laser and optical benches to prevent the light reflected by the interferometer and injection optical components from going back into the laser. In addition, the in-vacuum input mode cleaner cavity (IMC) control loops can be disturbed by the light back reflected by the interferometer that is scattered inside the IMC, and interferes with the forward travelling beam. Therefore, an additional optical isolation is achieved by placing an FI inside the vacuum vessel, between the IMC and the interferometer, to prevent the interferometer backreflected light to get into the IMC. This FI is operating in a 10^{-6} mbar vacuum environment, and it has to accommodate a beam having a several millimeter diameter size and several Watts of power. Owing to the quite large light intensity in the FI crystal, thermally induced effects in the FI were expected and observed, as thermal lensing [5], with consequent beam/interferometer mismatching, and optical isolation degradation ([6–8]). Reference [9] reports on the first observation of a further, formerly unexpected at this level, significant change of the optical isolation of an FI, which, having been tuned in air, once put in vacuum, experiences an isolation loss exceeding 10 dB. An explanation of this effect in terms of different heating of the terbium gallium garnet (TGG) crystal by the incoming beam when passing from air to vacuum, where the thermal dissipation of the air convection is absent, matches the observations [9]. The optical isolation degradation observed in Virgo, if not seriously affecting the interferometer at the time of its observation, has become more important after the Virgo + upgrades, where a larger amount of power is employed. The isolation loss depends also on the input power: because the interferometer must operate with different input powers, also depending on the interferometer locking conditions, precompensation by tuning the FI in air, in such a way that once in vacuum it will reach the maximum isolation, is not the best solution. The possibility to perform a fine tuning of the isolation once the FI is in vacuum is rather preferred. For this

0003-6935/10/254780-11$15.00/0

purpose, a dedicated remotely actuated system has been implemented in Virgo and successfully operated.

2. Verdet Constant Change Due to Laser Beam Heating

A. Faraday Isolator Isolation Degradation

Let us consider a FI as shown in Fig. 2(a): a Faraday rotator crystal (typically made of TGG in a magnetic field), rotating the input linear polarization by about 45°, is placed between two linear polarizers. The angle of the light impinging on the first polarizer ($\theta_0 = 0°$) is taken as a reference angle for the light polarization. We define $\theta_{FI} = 45° - \varepsilon$ as the rotation angle induced by the Faraday rotator. If the second polarizer axis is rotated by $\theta_{P2} = 45° + \alpha$ with respect to the reference angle θ_0, only the θ_{P2} polarization component of the light coming out from the FI rotator is transmitted by the second polarizer, any other component being reflected away. Thus,

$$\theta_{\mathrm{Back}} = \theta_{P2} + \theta_{\mathrm{FI}} = 45° + \alpha + 45° - \varepsilon, \tag{1}$$

where θ_{Back} is the polarization angle of the light coming back through the FI to the first input polarizer. If $\alpha = \varepsilon$ [Fig. 2(a)],

$$\theta_{\mathrm{Back}} = 90°, \tag{2}$$

and the light coming back, being cross polarized with respect to the input polarizer, is rejected by the FI. It must be observed that the second polarizer axis makes the polarization direction coincident with the one needed by the optical system downstream from the FI system. The optical isolation optimization obtained using the second polarizer happens at the expense of some light loss at the level of the second output polarizer, where the polarization of the impinging light differs by 2ε with respect to the second polarizer axis. A component 2ε is therefore reflected by the second polarizer. If the polarizer power reflection coefficient for the crossed polarization is $R(0°) = 1 - \sigma$ (and corresponding transmission $T(0°) = \sigma$), for small σ, the polarizer extinction power is

$$\frac{R(0°)}{T(0°)} = \frac{(1-\sigma)}{\sigma} \approx \frac{1}{\sigma}. \tag{3}$$

The fractional loss at the second polarizer as a function of the angle 2ε between the incident polarization and the polarizer axis is given by

$$\frac{T(2\varepsilon)}{R(2\varepsilon)} = \frac{(1-\sigma)\cos^2(2\varepsilon) + \sigma\sin^2(2\varepsilon)}{(1-\sigma)\sin^2(2\varepsilon) + \sigma\cos^2(2\varepsilon)}. \tag{4}$$

In the ideal conditions of perfectly linearly polarized input light, the optical isolation of the FI is limited essentially by the polarizer extinction σ, the maximum achievable optical isolation being given, for high polarizer extinction, by $T(90°)/R(90°) \approx 1/\sigma$.

What happens going from air to vacuum is shown in Fig. 2(b): the additional polarization rotation change η is introduced by the Faraday rotator, once the FI is in vacuum as demonstrated in [9], so that $\theta_{\mathrm{FI}} = 45° - \varepsilon - \eta$. Additional losses are introduced at the level of the output polarizer, where the light arrives with an additional polarization rotation angle η, thus yielding

$$\theta_{P2} - \theta_{\mathrm{FI}} = (45° + \varepsilon) - (45° - \varepsilon - \eta) = 2\varepsilon + \eta, \tag{5}$$

and the respective fractional loss, according to Eq. (4) becomes

$$\frac{T(2\varepsilon+\eta)}{R(2\varepsilon+\eta)} = \frac{(1-\sigma)\cos^2(2\varepsilon+\eta) + \sigma\sin^2(2\varepsilon+\eta)}{(1-\sigma)\sin^2(2\varepsilon+\eta) + \sigma\cos^2(2\varepsilon+\eta)}. \tag{6}$$

But the worse effect is on the optical isolation because

$$\theta_{\mathrm{Back}} = \theta_{P2} + \theta_{\mathrm{FI}} = 45° + \varepsilon + 45° - \varepsilon - \eta, \tag{7}$$

which yields

$$\theta_{\mathrm{Back}} = 90° - \eta. \tag{8}$$

This means that the light coming back through the FI is no more cross polarized with respect to the input polarizer, and the optical isolation is consequently spoiled. In Fig. 3, the effect of the additional angle η on the optical isolation for several polarizer extinction $1/\sigma$ is shown (in the ideal case of perfectly linear light polarization).

B. Verdet Constant Change Estimation

As explained in [9], this loss of isolation is mainly induced by a Verdet constant change with temperature and by absence of convection heat dissipation. In air, in the presence of heat dissipation by convection, the temperature increase of the TGG, with 34 W laser total power (superposition of the back-and-forth traveling laser beams), is about 3.8 K [9]. Already with a basic vacuum, the temperature increase is larger. In high vacuum (10^{-6} mbar), neglecting contour effects caused by the Faraday housing, the power irradiated by the TGG crystal, P_0 at equilibrium at ambient temperature ($T_0 = 293$ K), is well approximated by the Stefan–Boltzmann equation law for radiation:

$$P_0 = A\gamma\sigma T_0^4, \tag{9}$$

where A is the total irradiating surface (for a cylindrical TGG crystal 18 mm long and 20 mm in diameter, $A = 0.00176\ \mathrm{m}^2$) and σ the Stefan–Boltzmann constant. The crystal emissivity γ can be estimated to about 0.85 [9], taking into account the fact that the TGG does not behave exactly like a black body. Hence, if the crystal is illuminated by a laser beam, and P_{abs} is the laser power absorbed by the crystal, the temperature of the TGG at the equilibrium will be

$$T_L = \left\{ \frac{P_{\mathrm{abs}} + P_0}{A\gamma\sigma} \right\}^{1/4}. \tag{10}$$

With 34 W laser power and 1600 ppm/cm absorption, the temperature increase ΔT with respect to no input laser power can be estimated as being about 11.5 K (some deviation from this behavior has to be expected, principally due to the fact that the Faraday aluminum housing reflects back to the crystal part of the irradiated energy by the TGG, thus contributing to its heating). Given a rotation angle induced $\theta = VnLB$ ($V =$ TGG Verdet constant, $n =$ TGG refraction index, $L =$ TGG rod length, $B =$ magnetci field), the change of the Faraday rotation angle is dominated by the Verdet constant variation with temperature:

$$\frac{d\theta}{dT} = \frac{dV}{dT} nLB = \frac{dV}{dT} \frac{\theta}{V}. \tag{11}$$

The term $dV/(VdT)$ is estimated in [10] to about 3.5×10^{-3}/K, the derivative of V with respect to temperature being inversely proportional to temperature. Therefore, A variation of temperature ΔT induces a rotation angle variation η equal to

$$\eta = \frac{d\theta}{dT} \Delta T = 3.5 \times 10^{-3} \theta \Delta T. \tag{12}$$

In our case, the Faraday rotation angle induced by the temperature variation is about 1.8°.

3. Faraday Optical Isolation Remote Tuning: Principle

The reduced level of isolation significantly affects the interferometer performance, the disturbance becoming larger with the detector upgrade to an increased input power. For this reason, a possibility of remotely tuning the FI optical isolation has become necessary. A system able to perform remotely in vacuum the operations that are normally performed in air by an operator would require the motorization of many components of the optical isolator. A less-invasive system implies the introduction of additional optics (a half-waveplate) and the remote actuation of only one degree of freedom. This system introduces some additional loss at the level of the second polarizer but has the advantage of being quite simple. As shown in Fig. 4, if an additional half-waveplate is placed between the first polarizer and the rotator, and if this waveplate axis is rotated by an angle ξ, the light polarization is rotated by the waveplate by $\theta_{\lambda/2} = 2\xi$. The polarization angle of the light coming back through the FI onto the input polarizer is

$$\begin{aligned} \theta_{\mathrm{Back}} &= \theta_{P2} + \theta_{\mathrm{FI}} - \theta_{\lambda/2} = (45° + \varepsilon) + 45° - \varepsilon - \eta - \theta_{\lambda/2} \\ &= 90° - \eta - \theta_{\lambda/2}. \end{aligned} \tag{13}$$

If ξ is chosen such that $\theta_{\lambda/2} + \eta = 0$, the light coming back after a complete round trip will have a polarization rotated by 90° with respect to the first (input) polarizer axis and will be correctly reflected away [it could be observed that the same result would be obtained by placing the half-waveplate between the rotator and the second (output) polarizer]. Because the second half-waveplate can be mounted on a vacuum-compatible motorized mount, its rotation angle can be tuned accurately, until a minimum in the backreflected light is attained. This result is obtained at the expense of an increase of the light power rejected by the second polarizer, which had been initially tuned for a different (expected) polarization coming out from the Faraday rotator.

4. Faraday Optical Isolation Remote Tuning: Implementation and Measurements

In the Virgo interferometer, the in-vacuum FI is placed between the 144 m long IMC and the interferometer on an in-vacuum suspended bench (Fig. 1). The FI is a commercial Electro-Optics Technology vacuum-compatible FI, with a 2 cm diameter × 1.8 cm long TGG crystal rod, placed in a magnetic field of about 1 T. The beam passing through it having a diameter of 5.3 mm, the clear aperture of the FI is 20 mm to avoid losses and diffraction problems. After the recent Virgo to Virgo + upgrades, the incoming power is of the order of 17 W. About the same amount of power (95%) is reflected back by the interferometer when the recycling mirror is aligned, and about 60% when the interferometer is locked and in science mode. The rotation power of the Faraday rotator is about 43.5°, i.e., the rotation defect angle ε is equal to 1.5°. Many tuning optimization operations are necessary to achieve the maximum isolation, which requires a good alignment, fine positioning and rotation of polarizers and waveplates, beam dumps positioning, etc. All these operations are performed by an operator, with the FI in air. As described in [9], after having tuned the FI in air, with the correct amount of power, once the FI is placed in vacuum, the isolation level drops by an amount exceeding 10 dB.

The setup of Fig. 4 has been first tested in laboratory and then installed in the Virgo interferometer,

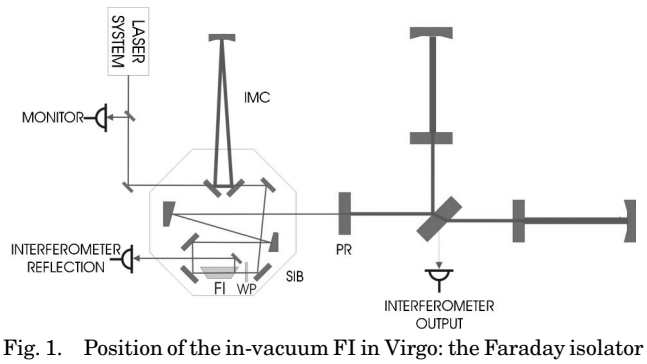

Fig. 1. Position of the in-vacuum FI in Virgo: the Faraday isolator (FI) is placed on the in-vacuum suspended injection bench (SIB), between the interferometer input (power recycling mirror, PR) and the input mode cleaner (IMC). The beam diameter at the level of the FI is about 5 mm, and the FI input power about 18 W.

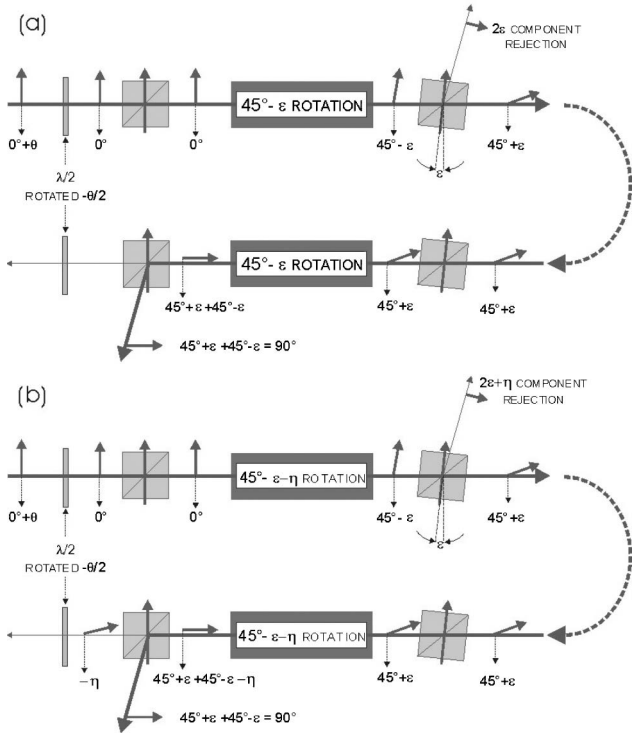

Fig. 2. (a) Realistic scheme of a FI setup, taking into account a Faraday rotator action of $45° - \varepsilon$ on the light polarization. The dashed line represents the coming back of the light after a round trip. (b) Faraday isolation is spoiled when going from air to vacuum. After being placed in vacuum, the rotation power of the Faraday rotator changes by an amount $-\eta$. The losses at the level of the second polarizer increase, and the polarization, after a round trip, is no more cross polarized with respect to the first polarizer: part of the light goes through the first polarizer toward the input. The FI optical isolation is spoiled.

as one of the upgrades included in the Virgo+ program. The same in-vacuum FI of Virgo is illuminated in a vacuum tank at the Virgo input power (17 W). The FI was tuned initially in air and then put in a vacuum. The rotated half-waveplate is a CVI QWPO-1064-10-2-R15, Nd:YAG, zero-order, high-power-vacuum compatible, antireflective coated ($R <$ 0.25%). The remotely commanded rotation stage selected for the $\lambda/2$ waveplate is a compact high-vacuum-compatible, Micos stepping motor rotation stage RS-40 SM, that is 20 mm thick and 650 g in weight. Typical resolution is 0.005° and unidirectional (bidirectional) repeatability is 0.005° (±0.04°). It is able to accommodate a 1 in. diameter waveplate, larger than the 20 mm Faraday rotator aperture (and TGG crystal diameter). In Virgo, owing to space constraints, it is not possible to place the waveplate rotator far from the Faraday magnet without severely affecting the very critical alignment of the suspended injection bench (SIB). Even when the waveplate rotator stepping motor movement is well calibrated and reproducible, if the mount is close to the FI magnet housing, the intense magnetic field of the Faraday magnet (of the order of 1 T) interacts with the motor, thus distorting the reading of the real motor rotation. In the first laboratory tests, the waveplate-motorized mount has been placed far from the Faraday magnet. In this case, going from air to a primary vacuum (residual pressure $>10^{-2}$ mbar), the isolation decreased from 41 dB (in air low-power tuning) down to 32.8 dB (with 39 W laser power). The isolation could be partially recovered by rotating the half-waveplate by 0.7°. The isolation reached was 36.5 dB. The discrepancy between the low-power maximum isolation and the maximum isolation we can get after having adjusted the half-waveplate at 39 W is due to thermal depolarization [7]. Taking into account a maximum achievable isolation of the FI of about 40 dB (even for low power and in air, the maximum isolation achieved has been less than 41 dB), the improvement in the isolation is in good agreement with Fig. 3, where a rotation angle of 0.7° of the waveplate corresponds to a compensation angle η of about 1.4° for polarizer losses $\sigma = 0.0001$. In Virgo configuration, the vacuum level is much better, and in this case it is sure that heat evacuation from magneto-optic crystals is only made by radiation. In the past [9], we have measured an isolation of the order of 30 dB for 20 W that we have estimated to be around 28 dB at 34 W. This corresponds to a polarization rotation angle η of about 2°, according to Fig. 3. This estimation is also in agreement with the prediction of Eq. (12), which would yield a variation η of the Faraday rotation angle of about 1.8° (assuming a TGG rotation angle of 43.5° and a temperature increase of the crystal, due to about 34 W laser illumination, of about 11.5 K). Tests with the waveplate closer to the Faraday magnet (up to 3 mm, as in the Virgo setup) give the same result in the optical isolation improvement, but the apparent rotation reading changes to several degrees. The comparison between the measurements far from and close to the magnet allows one to calibrate the motor rotation in the proximity of the FI magnetic field.

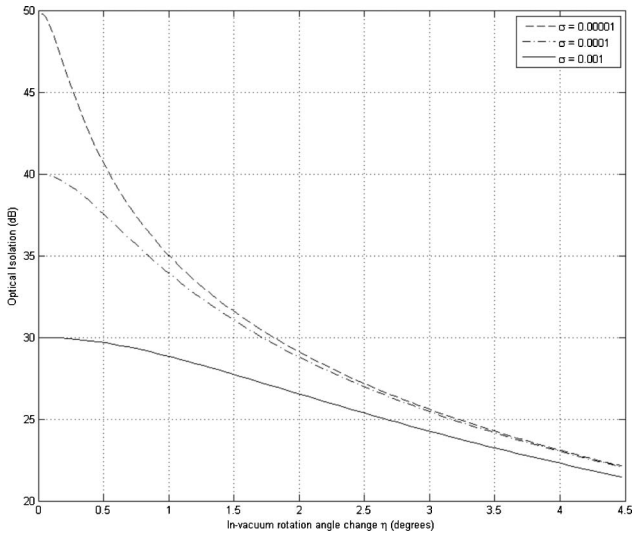

Fig. 3. Change of the optical isolation of the FI for different polarizer extinction values $1/\sigma$, as a function of the additional in-vacuum angle η (for perfectly linearly polarized light).

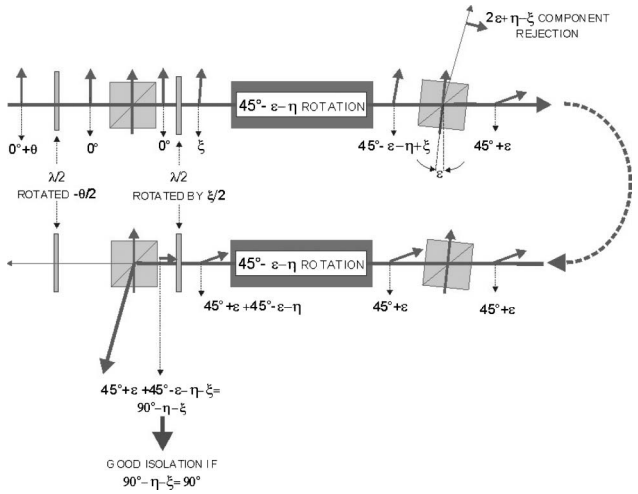

Fig. 4. Compensation of the in-vacuum reduced isolation level after additional half-waveplate. If a second half-waveplate is placed between the first polarizer and the Faraday rotator, the polarization of the light coming back after a round trip can be cross polarized with respect to the first polarizer if the waveplate is rotated by an angle $\xi/2 = -\eta/2$. The rotation of the waveplate can be finely tuned until the backreflection toward the input is minimized.

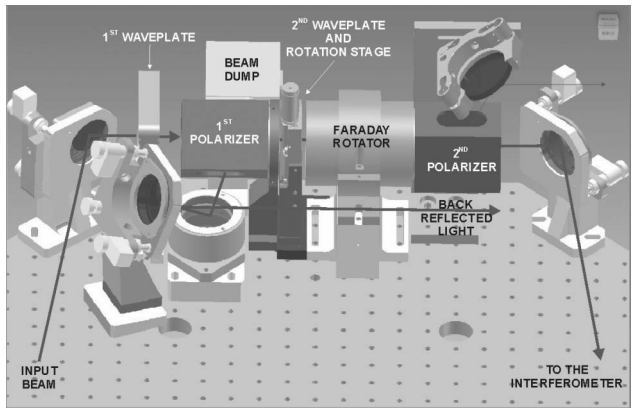

Fig. 5. Setup of the FI system on the Virgo SIB, with the additional waveplate: the remotely rotated half-waveplate is placed between the housing of the first (input) polarizer and the Faraday rotator. The light coming back from the interferometer is reflected away by the first polarizer toward a horizontal mirror and then picked up and sent outside the vacuum vessel by another mirror.

This effect, which was not expected in advance, has to be taken into account in future optical setups, namely in advanced interferometer upgrades in which the increase in the laser power will require more effective optical isolation and, consequently, larger FIs and likely larger magnetic fields. In Fig. 5, the complete Virgo setup is shown. As observed above, the additional half-waveplate could be placed either immediately before (upstream) or after (downstream) the Faraday rotator magnet housing. Owing to Virgo + space constraints, the best position was upstream of the Faraday rotator body, close to the FI magnet housing. The results obtained with the implementation of the Faraday isolation remote tuning are shown in Fig. 6. When the waveplate is rotated, the power reflected from the FI toward the external monitor (Monitor in Fig. 1) decreases. The optical isolation is computed accordingly, taking into account the known IMC transmitted power and the interferometer reflectivity. According to

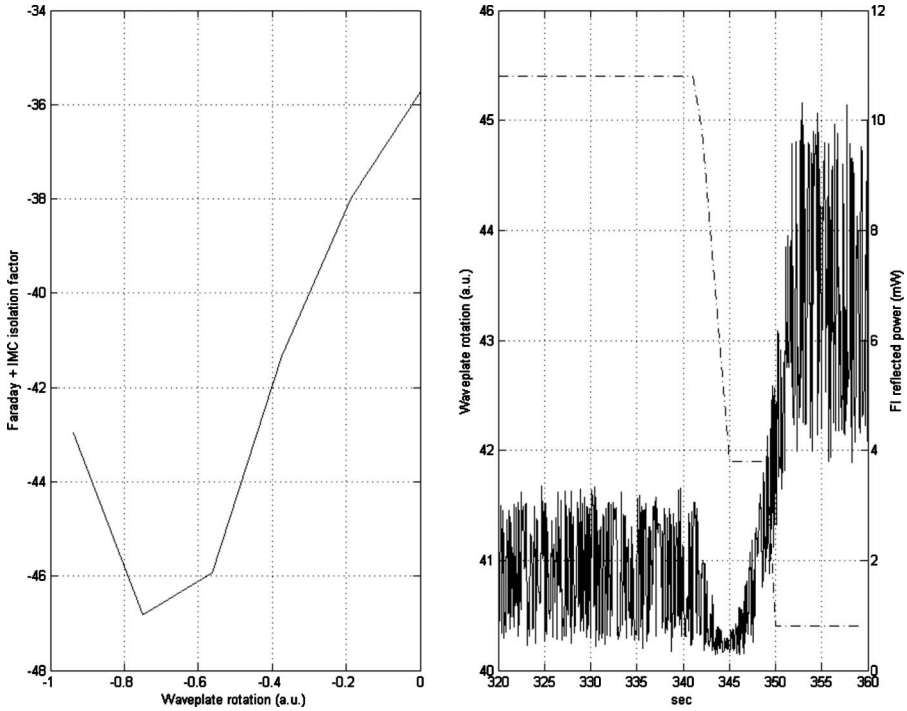

Fig. 6. Left: Evaluation of the optical isolation of the combined system FI and IMC. Right: Decrease of the power reflected back by the interferometer when rotating the waveplate; solid line, measured power; dash–Fdot line, waveplate rotation angle.

the measurements of Fig. 6, the final optical isolation of the FI would be almost 48 dB. This number is clearly overestimated. An exact measurement of the optical isolation in Virgo is complicated by the fact that the light coming back from the interferometer through the FI is measured by an external monitor (see Fig. 1). This light is coming back not only through the FI, but also through the IMC, so that the global isolation factor is given by the combination of the FI back transmission and the coupling with the IMC. The beam transmitted forward through the FI to the interferometer is not perfectly matched with the interferometer itself (mismatch being of the order of some percent), and the light coming back from the interferometer and transmitted toward the IMC by the FI is not perfectly matched with the IMC itself. Part of this light is a defocussed TEM_{00}, the defocussing being mainly due to thermal effects taking place in the FI (TGG + polarizers). This light component is dominant when the isolation of the FI is not optimized. The defocussing in the input polarizer is due to thermal effects in the BK7 polarizer substrate: even if the used polarizers (dielectric thin film Brewster polarizers) were tested as having a polarization extinction of better than 40 dB, the thin-film coating deposition process involves exposure to UV radiation. This exposure process is probably responsible for an increase in the absorption rate of the BK7, thus making thermal effects at high laser power in BK7 more significant [11]. This effect should be reduced once the BK7 polarizers are replaced by fused silica ones. Another part of the FI backtransmitted light is the residual light produced by thermally induced depolarization inside the FI TGG crystal, which has a non-TEM_{00} shape, as shown in Fig. 7. This component is the dominant one when the FI isolation is optimized, but it does not resonate inside the IMC cavity. The power measured by the monitor in Fig. 1 is, therefore, less than the effective one backtransmitted by the FI at the optimized isolation point, which can be assumed as being close to the 36.5 dB value measured in the laboratory setup. Depolarization in the

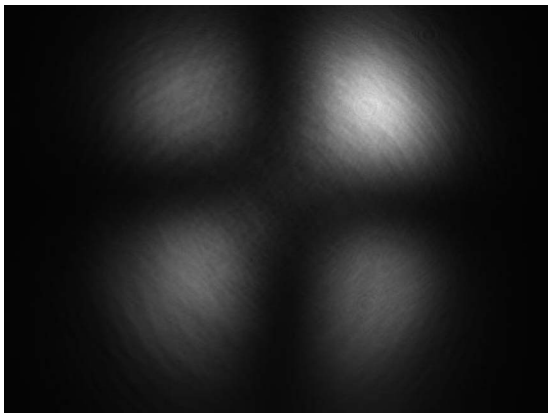

Fig. 7. Spatial profile of the depolarization light generated in the FI TGG crystal.

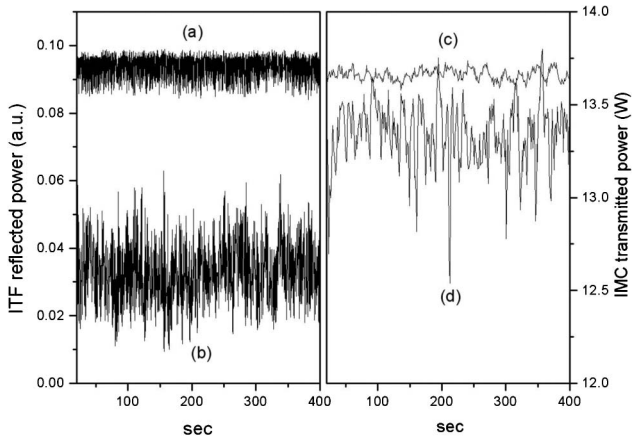

Fig. 8. Improvement in the interferometer signals: (left) The interferometer reflected power (a) after and (b) before FI optimization. (right) The IMC transmission (the light going into the interometer) (c) after and (d) before FI optimization. For the sake of clarity, an offset has been introduced between the two curves.

TGG becomes a limiting effect from 10 W laser power. It will limit the maximum optical isolation achievable by the FI. Even if it is difficult to obtain a precise measurement of the actual optical isolation achieved, the benefit for the interferometer behavior is clearly visible. Figure 8 shows the improvement in the IMC transmitted light and in the interferometer reflection. In both cases, the stability of the power delivered to the interferometer and of the reflected signal is improved. This stability improvement contributes to the global robustness of the Virgo interferometer and to the growth of the data-taking duty cycle, which is a crucial figure of the gravitational wave detector.

5. Conclusion

Thermal effects in FIs exposed to high input power, in particular when placed in vacuum, have only been intensively studied for a relatively short time. Some in-vacuum thermal effects have been recently observed in gravitational wave interferometers, including a degradation of the optical isolation when passing from air to vacuum. With the improvement of the interferometers sensitivity and the increase of the laser input power, the requirements on the optical isolation from backreflected light toward the injection system are becoming more demanding. The possibility to correct or compensate these thermal effects is, therefore, acquiring more relevance. In this paper, we have described a system able to compensate at least the drop in optical isolation consequent to the passage from air to vacuum of an in-air-tuned FI. It implies the introduction of an additional half-waveplate, whose rotation is finely controlled remotely. After the implementation in the Virgo gravitational wave interferometer, by a rotation of less than 1° of the half-waveplate, an optimization of the optical isolation of the optical isolation of the FI of several dB can be achieved. Besides the possibility to obtain fine tuning, the remote rotation of

the half-waveplate offers the advantage of adapting the system to the different power levels of the interferometer operation steps and allows one to operate with different input powers. The system is simple in principle and implementation and has proven to be effective, yielding significant advantage in the present higher level of input power operation of the Virgo interferometer.

Appendix A

T. Accadia is with the Laboratoire d'Annecy-le-Vieux de Physique des Particules (LAPP), IN2P3/CNRS, Université de Savoie, F-74941 Annecy-le-Vieux, France.

F. Acernese is with INFN, Sezione di , I-80126 , Italy and/or Università di Salerno, Fisciano, I-84084 Salerno, Italy.

F. Antonucci is with INFN, Sezione di Roma, I-00185 Roma, Italy.

S. Aoudia is with the Université Nice-Sophia-Antipolis, CNRS, Observatoire de la Côte d'Azur, F-06304 Nice, France.

K. G. Arun is with LAL, Université Paris-Sud, IN2P3/CNRS, F-91898 Orsay, France and/or ESPCI, CNRS, F-75005 Paris, France.

P. Astone is with the INFN, Sezione di Roma, I-00185 Roma, Italy.

G. Ballardin is with the European Gravitational Observatory (EGO), I-56021 Cascina (Pi), Italy.

F. Barone is with the INFN, Sezione di , I-80126 , Italy and/or Università di Salerno, Fisciano, I-84084 Salerno, Italy.

M. Barsuglia is with the AstroParticule et Cosmologie (APC), CNRS: UMR7164-IN2P3-Observatoire de Paris-Université Denis Diderot-Paris 7—CEA: DSM/IRFU, Paris, France.

Th. S. Bauer is with Nikhef, National Institute for Subatomic Physics, P.O. Box 41882, 1009 DB Amsterdam, The Netherlands.

M.G. Beker is with Nikhef, National Institute for Subatomic Physics, P.O. Box 41882, 1009 DB Amsterdam, The Netherlands.

S. Bigotta is with INFN, Sezione di Pisa, I-56100 Pisa, Italy and/or Università di Pisa, I-56127 Pisa, Italy.

S. Birindelli is with the Université Nice-Sophia-Antipolis, CNRS, Observatoire de la Côte d'Azur, F-06304 Nice, France.

M. Bitossi is with INFN, Sezione di Pisa, I-56100 Pisa, Italy.

M. A. Bizouard is with the LAL, Université Paris-Sud, IN2P3/CNRS, F-91898 Orsay, France.

M. Blom is with the Nikhef, National Institute for Subatomic Physics, P.O. Box 41882, 1009 DB Amsterdam, The Netherlands.

C. Boccara is with the ESPCI, CNRS, F-75005 Paris, France.

F. Bondu is with the Institut de Physique de Rennes, CNRS, Université de Rennes 1, 35042 Rennes, France.

L. Bonelli is with the INFN, Sezione di Pisa, I-56100 Pisa, Italy and/or Università di Pisa, I-56127 Pisa, Italy.

L. Bosi is with the INFN, Sezione di Perugia, I-6123 Perugia, Italy.

S. Braccini is with the INFN, Sezione di Pisa, I-56100 Pisa, Italy.

C. Bradaschia is with the INFN, Sezione di Pisa, I-56100 Pisa, Italy.

A. Brillet is with the Université Nice-Sophia-Antipolis, CNRS, Observatoire de la Côte d'Azur, F-06304 Nice, France.

V. Brisson is with the LAL, Université Paris-Sud, IN2P3/CNRS, F-91898 Orsay, France.

R. Budzynski is with Warsaw University, 00-681 Warsaw, Poland.

T. Bulik is with the Warsaw University Astronomical Observatory , 00-478 Warsaw, Poland and/or CAMK-PAN, 00-716 Warsaw, Poland.

H. J. Bulten is with Nikhef, National Institute for Subatomic Physics, P.O. Box 41882, 1009 DB Amsterdam, The Netherlands and/or VU University Amsterdam, De Boelelaan 1081, 1081 HV Amsterdam, The Netherlands.

D. Buskulic is with the Laboratoire d'Annecy-le-Vieux de Physique des Particules (LAPP), IN2P3/CNRS, Université de Savoie, F-74941 Annecy-le-Vieux, France.

G. Cagnoli is with the INFN, Sezione di Firenze, I-50019 Sesto Fiorentino, Italy.

E. Calloni is with the INFN, Sezione di , I-80126 , Italy and/or Università di 'Federico II,' Complesso Universitario di Monte S. Angelo, I-80126 , Italy.

E. Campagna is with the INFN, Sezione di Firenze, I-50019 Sesto Fiorentino, Italy and/or Università degli Studi di Urbino 'Carlo Bo,' I-61029 Urbino, Italy.

B. Canuel is with the European Gravitational Observatory (EGO), I-56021 Cascina (Pi), Italy.

F. Carbognani is with the European Gravitational Observatory (EGO), I-56021 Cascina (Pi), Italy.

F. Cavalier is with the LAL, Université Paris-Sud, IN2P3/CNRS, F-91898 Orsay, France.

R. Cavalieri is with the European Gravitational Observatory (EGO), I-56021 Cascina (Pi), Italy.

G. Cella is with the INFN, Sezione di Pisa, I-56100 Pisa, Italy.

E. Cesarini is with the Università degli Studi di Urbino 'Carlo Bo,' I-61029 Urbino, Italy.

E. Chassande-Mottin is with the AstroParticule et Cosmologie (APC), CNRS: UMR7164-IN2P3-Observatoire de Paris-Université Denis Diderot-Paris 7—CEA:DSM/IRFU, Paris, France.

A. Chincarini is with the INFN, Sezione di Genova; I-16146 Genova, Italy.

F. Cleva is with the Université Nice-Sophia-Antipolis, CNRS, Observatoire de la Côte d'Azur, F-06304 Nice, France.

E. Coccia is with the INFN, Sezione di Roma Tor Vergata, I-67100 Roma, Italy and/or Università di Roma Tor Vergata, I-67100 Roma, Italy.

C. N. Colacino is with the INFN, Sezione di Pisa, I-56100 Pisa, Italy.

J. Colas is with the European Gravitational Observatory (EGO), I-56021 Cascina (Pi), Italy.

A. Colla is with the INFN, Sezione di Roma, I-00185 Roma, Italy and/or Università 'La Sapienza,' I-00185 Roma, Italy.

M. Colombini is with the Università 'La Sapienza,' I-00185 Roma, Italy.

C. Corda is with the INFN, Sezione di Pisa, I-56100 Pisa, Italy and/or Università di Pisa, I-56127 Pisa, Italy.

A. Corsi is with the INFN, Sezione di Roma, I-00185 Roma, Italy.

J.-P. Coulon is with the Université Nice-Sophia-Antipolis, CNRS, Observatoire de la Côte d'Azur, F-06304 Nice, France.

E. Cuoco is with the European Gravitational Observatory (EGO), I-56021 Cascina (Pi), Italy.

S. D'Antonio is with the INFN, Sezione di Roma Tor Vergata, I-67100 Roma, Italy.

A. Dari is with the INFN, Sezione di Perugia, I-6123 Perugia, Italy and/or Università di Perugia, I-6123 Perugia, Italy.

V. Dattilo is with the European Gravitational Observatory (EGO), I-56021 Cascina (Pi), Italy.

M. Davier is with the LAL, Université Paris-Sud, IN2P3/CNRS, F-91898 Orsay, France.

R. Day is with the European Gravitational Observatory (EGO), I-56021 Cascina (Pi), Italy.

R. De Rosa is with the INFN, Sezione di, I-80126, Italy and/or Università di 'Federico II,' Complesso Universitario di Monte S. Angelo, I-80126, Italy.

M. del Prete is with the INFN, Sezione di Pisa, I-56100 Pisa, Italy and/or Università di Siena, I-53100 Siena, Italy.

L. Di Fiore is with the INFN, Sezione di, I-80126, Italy.

A. Di Lieto is with the INFN, Sezione di Pisa, I-56100 Pisa, Italy and/or Università di Pisa, I-56127 Pisa, Italy.

M. Di Paolo Emilio is with the INFN, Sezione di Roma Tor Vergata, I-67100 Roma, Italy and/or Università dell'Aquila, I-67100 L'Aquila, Italy.

A. Di Virgilio is with the INFN, Sezione di Pisa, I-56100 Pisa, Italy.

A. Dietz is with the Laboratoire d'Annecy-le-Vieux de Physique des Particules (LAPP), IN2P3/CNRS, Université de Savoie, F-74941 Annecy-le-Vieux, France.

M. Drago is with the INFN, Sezione di Padova, I-35131 Padova, Italy and/or Università di Padova, I-35131 Padova, Italy.

V. Fafone is with the INFN, Sezione di Roma Tor Vergata, I-67100 Roma, Italy and/or Università di Roma Tor Vergata, I-67100 Roma, Italy.

I. Ferrante is with the INFN, Sezione di Pisa, I-56100 Pisa, Italy and/or Università di Pisa, I-56127 Pisa, Italy.

F. Fidecaro is with the INFN, Sezione di Pisa, I-56100 Pisa, Italy and/or Università di Pisa, I-56127 Pisa, Italy.

I. Fiori is with the European Gravitational Observatory (EGO), I-56021 Cascina (Pi), Italy.

R. Flaminio is with the Laboratoire des Matériaux Avancés (LMA), IN2P3/CNRS, F-69622 Villeurbanne, Lyon, France.

J.-D. Fournier is with the Université Nice-Sophia-Antipolis, CNRS, Observatoire de la Côte d'Azur, F-06304 Nice, France.

J. Franc is with the Laboratoire des Matériaux Avancés (LMA), IN2P3/CNRS, F-69622 Villeurbanne, Lyon, France.

S. Frasca is with the INFN, Sezione di Roma, I-00185 Roma, Italy and/or Università 'La Sapienza,' I-00185 Roma, Italy.

F. Frasconi is with the INFN, Sezione di Pisa, I-56100 Pisa, Italy.

A. Freise is with the University of Birmingham, Birmingham, B15 2TT, United Kingdom.

L. Gammaitoni is with the INFN, Sezione di Perugia, I-6123 Perugia, Italy and/or Università di Perugia, I-6123 Perugia, Italy.

F. Garufi is with the INFN, Sezione di , I-80126 , Italy and/or Università di 'Federico II,' Complesso Universitario di Monte S. Angelo, I-80126 , Italy.

G. Gemme is with the INFN, Sezione di Genova; I-16146 Genova, Italy.

E. Genin is with the European Gravitational Observatory (EGO), I-56021 Cascina (Pi), Italy.

A. Gennai is with the INFN, Sezione di Pisa, I-56100 Pisa, Italy.

A. Giazotto is with the INFN, Sezione di Pisa, I-56100 Pisa, Italy.

R. Gouaty is with the Laboratoire d'Annecy-le-Vieux de Physique des Particules (LAPP), IN2P3/CNRS, Université de Savoie, F-74941 Annecy-le-Vieux, France.

M. Granata is with the AstroParticule et Cosmologie (APC), CNRS: UMR7164-IN2P3-Observatoire de Paris-Université Denis Diderot-Paris 7—CEA:DSM/IRFU, Paris, France.

C. Greverie is with the Université Nice-Sophia-Antipolis, CNRS, Observatoire de la Côte d'Azur, F-06304 Nice, France.

G. M. Guidi is with the INFN, Sezione di Firenze, I-50019 Sesto Fiorentino, Italy and/or Università degli Studi di Urbino 'Carlo Bo,' I-61029 Urbino, Italy.

H. Heitmann is with the Université Nice-Sophia-Antipolis, CNRS, Observatoire de la Côte d'Azur, F-06304 Nice, France and/or Institut de Physique de Rennes, CNRS, Université de Rennes 1, 35042 Rennes, France.

P. Hello is with the LAL, Université Paris-Sud, IN2P3/CNRS, F-91898 Orsay, France.

S. Hild is with the University of Glasgow, Glasgow, G12 8QQ, United Kingdom.

D. Huet is with the European Gravitational Observatory (EGO), I-56021 Cascina (Pi), Italy.

P. Jaranowski is with the Bialystok University, 15-424 Bialystok, Poland.

I. Kowalska is with the Warsaw University Astronomical Observatory , 00-478 Warsaw, Poland.

A. Królak is with the IM-PAN, 00-956 Warsaw, Poland and/or IPJ, 05-400 Świerk-Otwock, Poland.

P. La Penna is with the European Gravitational Observatory (EGO), I-56021 Cascina (Pi), Italy.

N. Leroy is with the LAL, Université Paris-Sud, IN2P3/CNRS, F-91898 Orsay, France.

N. Letendre is with the Laboratoire d'Annecy-le-Vieux de Physique des Particules (LAPP), IN2P3/CNRS, Université de Savoie, F-74941 Annecy-le-Vieux, France.

T. G. F. Li is with the Nikhef, National Institute for Subatomic Physics, P.O. Box 41882, 1009 DB Amsterdam, The Netherlands.

M. Lorenzini is with the INFN, Sezione di Firenze, I-50019 Sesto Fiorentino, Italy.

V. Loriette is with the ESPCI, CNRS, F-75005 Paris, France.

G. Losurdo is with the INFN, Sezione di Firenze, I-50019 Sesto Fiorentino, Italy.

J. M. Mackowski is with the Laboratoire des Matériaux Avancés (LMA), IN2P3/CNRS, F-69622 Villeurbanne, Lyon, France.

E. Majorana is with the INFN, Sezione di Roma, I-00185 Roma, Italy.

N. Man is with the Université Nice-Sophia-Antipolis, CNRS, Observatoire de la Côte d'Azur, F-06304 Nice, France.

M. Mantovani is with the INFN, Sezione di Pisa, I-56100 Pisa, Italy and/or Università di Siena, I-53100 Siena, Italy.

F. Marchesoni is with the INFN, Sezione di Perugia, I-6123 Perugia, Italy.

F. Marion is with the Laboratoire d'Annecy-le-Vieux de Physique des Particules (LAPP), IN2P3/CNRS, Université de Savoie, F-74941 Annecy-le-Vieux, France.

J. Marque is with the European Gravitational Observatory (EGO), I-56021 Cascina (Pi), Italy.

F. Martelli is with the INFN, Sezione di Firenze, I-50019 Sesto Fiorentino, Italy and/or Università degli Studi di Urbino 'Carlo Bo,' I-61029 Urbino, Italy.

A. Masserot is with the Laboratoire d'Annecy-le-Vieux de Physique des Particules (LAPP), IN2P3/CNRS, Université de Savoie, F-74941 Annecy-le-Vieux, France.

C. Michel is with the Laboratoire des Matériaux Avancés (LMA), IN2P3/CNRS, F-69622 Villeurbanne, Lyon, France.

L. Milano is with the INFN, Sezione di , I-80126 , Italy and/or Università di 'Federico II,' Complesso Universitario di Monte S. Angelo, I-80126 , Italy.

Y. Minenkov is with the INFN, Sezione di Roma Tor Vergata, I-67100 Roma, Italy.

M. Mohan is with the European Gravitational Observatory (EGO), I-56021 Cascina (Pi), Italy.

J. Moreau is with the ESPCI, CNRS, F-75005 Paris, France.

N. Morgado is with the Laboratoire des Matériaux Avancés (LMA), IN2P3/CNRS, F-69622 Villeurbanne, Lyon, France.

A. Morgia is with the INFN, Sezione di Roma Tor Vergata, I-67100 Roma, Italy and/or Università di Roma Tor Vergata, I-67100 Roma, Italy.

S. Mosca is with the INFN, Sezione di , I-80126 , Italy and/or Università di 'Federico II,' Complesso Universitario di Monte S. Angelo, I-80126 , Italy.

V. Moscatelli is with the INFN, Sezione di Roma, I-00185 Roma, Italy.

B. Mours is with the Laboratoire d'Annecy-le-Vieux de Physique des Particules (LAPP), IN2P3/CNRS, Université de Savoie, F-74941 Annecy-le-Vieux, France.

I. Neri is with the INFN, Sezione di Perugia, I-6123 Perugia, Italy and/or Università di Perugia, I-6123 Perugia, Italy.

F. Nocera is with the European Gravitational Observatory (EGO), I-56021 Cascina (Pi), Italy.

G. Pagliaroli is with the INFN, Sezione di Roma Tor Vergata, I-67100 Roma, Italy and/or Università dell'Aquila, I-67100 L'Aquila, Italy.

L. Palladino is with the INFN, Sezione di Roma Tor Vergata, I-67100 Roma, Italy and/or Università dell'Aquila, I-67100 L'Aquila, Italy.

C. Palomba is with the INFN, Sezione di Roma, I-00185 Roma, Italy.

F. Paoletti is with the INFN, Sezione di Pisa, I-56100 Pisa, Italy and/or European Gravitational Observatory (EGO), I-56021 Cascina (Pi), Italy.

, S. Pardi is with the INFN, Sezione di , I-80126 , Italy and/or Università di 'Federico II,' Complesso Universitario di Monte S. Angelo, I-80126 , Italy.

M. Parisi is with the Università di 'Federico II,' Complesso Universitario di Monte S. Angelo, I-80126 , Italy.

A. Pasqualetti is with the European Gravitational Observatory (EGO), I-56021 Cascina (Pi), Italy.

R. Passaquieti is with the INFN, Sezione di Pisa, I-56100 Pisa, Italy and/or Università di Pisa, I-56127 Pisa, Italy.

D. Passuello is with the INFN, Sezione di Pisa, I-56100 Pisa, Italy.

G. Persichetti is with the INFN, Sezione di, I-80126, Italy and/or Università di 'Federico II,' Complesso Universitario di Monte S. Angelo, I-80126, Italy.

M. Pichot is with the Université Nice-Sophia-Antipolis, CNRS, Observatoire de la Côte d'Azur, F-06304 Nice, France.

F. Piergiovanni is with the INFN, Sezione di Firenze, I-50019 Sesto Fiorentino, Italy and/or Università degli Studi di Urbino 'Carlo Bo,' I-61029 Urbino, Italy.

M. Pietka is with the Bialystok University, 15-424 Bialystok, Poland.

L. Pinard is with the Laboratoire des Matériaux Avancés (LMA), IN2P3/CNRS, F-69622 Villeurbanne, Lyon, France.

R. Poggiani is with the INFN, Sezione di Pisa, I-56100 Pisa, Italy and/or Università di Pisa, I-56127 Pisa, Italy.

M. Prato is with the INFN, Sezione di Genova; I-16146 Genova, Italy.

G. A. Prodi is with the INFN, Gruppo Collegato di Trento, I-38050 Povo, Trento, Italy and/or Università di Trento, I-38050 Povo, Trento, Italy.

M. Punturo is with the INFN, Sezione di Perugia, I-6123 Perugia, Italy.

P. Puppo is with the INFN, Sezione di Roma, I-00185 Roma, Italy.

O. Rabaste is with the AstroParticule et Cosmologie (APC), CNRS: UMR7164-IN2P3-Observatoire de Paris-Université Denis Diderot-Paris 7—CEA:DSM/IRFU, Paris, France.

D. S. Rabeling is with Nikhef, National Institute for Subatomic Physics, P.O. Box 41882, 1009 DB Amsterdam, The Netherlands and/or VU University Amsterdam, De Boelelaan 1081, 1081 HV Amsterdam, The Netherlands.

P. Rapagnani is with the INFN, Sezione di Roma, I-00185 Roma, Italy and/or Università 'La Sapienza,' I-00185 Roma, Italy.

V. Re is with the INFN, Gruppo Collegato di Trento, I-38050 Povo, Trento, Italy and/or Università di Trento, I-38050 Povo, Trento, Italy.

T. Regimbau is with the Université Nice-Sophia-Antipolis, CNRS, Observatoire de la Côte d'Azur, F-06304 Nice, France.

F. Ricci is with the INFN, Sezione di Roma, I-00185 Roma, Italy and/or Università 'La Sapienza,' I-00185 Roma, Italy.

F. Robinet is with the LAL, Université Paris-Sud, IN2P3/CNRS, F-91898 Orsay, France.

A. Rocchi is with the INFN, Sezione di Roma Tor Vergata, I-67100 Roma, Italy.

L. Rolland is with the Laboratoire d'Annecy-le-Vieux de Physique des Particules (LAPP), IN2P3/CNRS, Université de Savoie, F-74941 Annecy-le-Vieux, France.

R. Romano is with the INFN, Sezione di, I-80126, Italy and/or Università di 'Federico II,' Complesso Universitario di Monte S. Angelo, I-80126 , Italy.

D. Rosińska is with the Institute of Astronomy, 65-265 Zielona Góra, Poland.

P. Ruggi is with the European Gravitational Observatory (EGO), I-56021 Cascina (Pi), Italy.

B. Sassolas is with the Laboratoire des Matériaux Avancés (LMA), IN2P3/CNRS, F-69622 Villeurbanne, Lyon, France.

D. Sentenac is with the European Gravitational Observatory (EGO), I-56021 Cascina (Pi), Italy.

R. Sturani is with the INFN, Sezione di Firenze, I-50019 Sesto Fiorentino, Italy and/or Università degli Studi di Urbino 'Carlo Bo,' I-61029 Urbino, Italy.

B. Swinkels is with the European Gravitational Observatory (EGO), I-56021 Cascina (Pi), Italy.

A. Toncelli is with the INFN, Sezione di Pisa, I-56100 Pisa, Italy and/or Università di Pisa, I-56127 Pisa, Italy.

M. Tonelli is with the INFN, Sezione di Pisa, I-56100 Pisa, Italy and/or Università di Pisa, I-56127 Pisa, Italy.

E. Tournefier is with the Laboratoire d'Annecy-le-Vieux de Physique des Particules (LAPP), IN2P3/CNRS, Université de Savoie, F-74941 Annecy-le-Vieux, France.

F. Travasso is with the INFN, Sezione di Perugia, I-6123 Perugia, Italy and/or Università di Perugia, I-6123 Perugia, Italy.

J. Trummer is with the Laboratoire d'Annecy-le-Vieux de Physique des Particules (LAPP), IN2P3/CNRS, Université de Savoie, F-74941 Annecy-le-Vieux, France.

G. Vajentei is with the INFN, Sezione di Pisa, I-56100 Pisa, Italy and/or Università di Pisa, I-56127 Pisa, Italy.

J. F. J. van den Brand is with Nikhef, National Institute for Subatomic Physics, P.O. Box 41882, 1009 DB Amsterdam, The Netherlands and/or VU University Amsterdam, De Boelelaan 1081, 1081 HV Amsterdam, The Netherlands.

S. van der Putten is with Nikhef, National Institute for Subatomic Physics, P.O. Box 41882, 1009 DB Amsterdam, The Netherlands.

M. Vavoulidis is with the LAL, Université Paris-Sud, IN2P3/CNRS, F-91898 Orsay, France.

G. Vedovato is with the INFN, Sezione di Padova, I-35131 Padova, Italy.

D. Verkindt is with the Laboratoire d'Annecy-le-Vieux de Physique des Particules (LAPP), IN2P3/CNRS, Université de Savoie, F-74941 Annecy-le-Vieux, France.

F. Vetrano is with the INFN, Sezione di Firenze, I-50019 Sesto Fiorentino, Italy and/or Università degli Studi di Urbino 'Carlo Bo,' I-61029 Urbino, Italy.

A. Viceré is with the INFN, Sezione di Firenze, I-50019 Sesto Fiorentino, Italy and/or Università degli Studi di Urbino 'Carlo Bo,' I-61029 Urbino, Italy.

J.-Y. Vinet is with the Université Nice-Sophia-Antipolis, CNRS, Observatoire de la Côte d'Azur, F-06304 Nice, France.

H. Vocca is with the INFN, Sezione di Perugia, I-6123 Perugia, Italy.

M. Was is with the LAL, Université Paris-Sud, IN2P3/CNRS, F-91898 Orsay, France.

M. Yvert is with the Laboratoire d'Annecy-le-Vieux de Physique des Particules (LAPP), IN2P3/CNRS, Université de Savoie, F-74941 Annecy-le-Vieux, France.

References

1. The Virgo Collaboration, "Virgo status," Class. Quantum Grav. **25**, 184001 (2008).
2. The Ligo Collaboration, "Status of the Ligo detectors," Class. Quantum Grav. **25**, 114041 (2008).
3. The GEO Collaboration, "The Geo–HF project," Class. Quantum Grav. **23**, S207–S214 (2006).
4. The TAMA Collaboration, "Status of TAMA300," Class. Quantum Grav. **21**, S403–S408 (2004).
5. J. D. Mansell, J. Hennawi, E. K. Gustafson, M. M. Fejer, R. L. Byer, D. Clubley, S. Yoshida, and D. H. Reitze, "Evaluation the effect of transmissive optic thermal lensing on laser

beam quality with a Shack–Hartmann wave-front sensor," Appl. Opt. **40**, 366–374 (2001).
6. E. A. Khazanov, A. Poteomkin, V. Zelenogorsky, A. Shaykin, A. Mal'shakov, O. Palashov, and D. H. Reitze, "Adaptive compensation of thermal lens in Faraday isolators," Proc. SPIE **5332**, 271–282 (2004).
7. E. A. Khazanov, O. V. Kulagin, S. Yoshida, D. B. Tanner, and D. H. Reitze, "Investigation of self-induced depolarization of laser radiation in terbium gallium garnet," IEEE J. Quantum Electron. **35**, 1116–1122 (1999).
8. V. V. Zelenogorsky, E. E. Kamenetsky, A. A. Shaykin, O. V. Palashov, and E. A. Khazanov, "Adaptive compensation of thermally induced aberrations in Faraday isolator by means of a DKDP crystal," Proc. SPIE **5975**, 59750I (2006).
9. The Virgo Collaboration, "In-vacuum optical isolation changes by heating in a Faraday isolator," Appl. Opt. **47**, 5853–5861 (2008).
10. N. P. Barnes and L. B. Petway, "Variation of Verdet constant with temperature in terbium gallium garnet," J. Opt. Soc. Am. B **9**, 1912–1915(1992).
11. A. Gatto, L. Escoubas, P. Roche, and M. Commandré, "Simulation of the degradation of optical glass substrates caused by UV irradiation while coating," Opt. Commun. **148**, 347–354 (1998).